

Emergence of the periodic oscillatory modulation in time-like nucleon form factors

Ri-Qing Qian^{1,2,3,*}, Zhan-Wei Liu^{1,2,3,†}, Xu Cao^{2,3,4,5,‡} and Xiang Liu^{1,2,3,§}

¹*School of Physical Science and Technology, Lanzhou University, Lanzhou 730000, China*

²*Research Center for Hadron and CSR Physics, Lanzhou University
and Institute of Modern Physics of CAS, Lanzhou 730000, China*

³*Lanzhou Center for Theoretical Physics, Key Laboratory of Theoretical Physics of Gansu Province
and Frontier Science Center for Rare Isotopes, Lanzhou University, Lanzhou 730000, China*

⁴*Institute of Modern Physics, Chinese Academy of Sciences, Lanzhou 730000, China*

⁵*University of Chinese Academy of Sciences, Beijing 100049, China*

We have studied the oscillatory behavior exhibited in the timelike electromagnetic form factors of nucleons by considering the final-state interaction effect. This mechanism introduces the Jost function of $N\bar{N}$ pair into the time-like form factors with the help of the distorted-wave Born approximation. Using a simple square-well potential, the contribution from the final-state interaction in our approach is naturally damped oscillatory, which can explain the experimental data very nicely. This scenario seems to be universal considering that it also reproduces well the threshold enhancements on the cross sections for $e^+e^- \rightarrow n\bar{n}$, $\Lambda\bar{\Lambda}$, and $\Lambda_c\bar{\Lambda}_c$.

Introduction.— Nucleon electromagnetic form factors are of fundamental interest with the aim to understand the internal structure of this subatomic entity. They describe the couplings of virtual photon with nucleon electromagnetic currents, which are related to the dynamical properties of internal quarks and gluons. The form factors in the space-like region were obtained from precise electron-nucleon scattering data with large statistics [1, 2], while the time-like ones were measured in the e^+e^- annihilation process [3–6]. These are analytically connected and can be simultaneously studied within the vector-meson-dominance models [7–11], dispersion approaches [12, 13], perturbative QCD parametrization [14, 15], chiral perturbation theory [16–18], and so on (See Ref. [19] for recent review).

Precise experimental measurements show unexpected oscillation behavior of time-like form factors for protons in the near-threshold region [5, 20]. Similar oscillation phenomenon was also observed for neutrons [6, 21]. The effective form factors G_{eff} of nucleons can be divided into two parts. The main part G^0 can be obtained with a perturbative QCD parametrization and describe the main decreasing behavior of the form factor very well while the remaining one G^{osc} exhibits a damped oscillation with regularly spaced maxima and minimum over sub-GeV scale [20].

The oscillatory behavior was firstly pointed out in Ref. [20] and has been studied in different approaches [22–26]. The crests and troughs of the oscillation pattern may be explained by introducing a few meson resonances [22–24], and it is mentioned that the threshold cusps from hadron-antihadron channels may also contribute [24].

A good separation of damped oscillatory part from a smooth part indicates two different intrinsic mechanisms. Natural speculation is that these two correspond to the bare formation of $N\bar{N}$ and the rescattering of the $N\bar{N}$ pair with the final-state interaction (FSI) [20]. It is shown

in Ref. [25] that the qualitative feature of the oscillation can be produced with a complicated optical potential of $N\bar{N}$ FSI. The role of soft rescattering on time-like proton form factors was discussed based on its physical interpretation similar to the charge distribution of space-like ones [27, 28]. Other considerations of FSI can explain the near-threshold enhancement [26, 29], which is the reflection of the first maximum of the oscillation behavior.

So far a complete and plausible understanding of the emergence of oscillation behavior is still missing. A more natural explanation is needed for the observed good periodicity.

In the present work, we focus on how FSI leads to the oscillatory behavior with proper separation between the formation and FSI processes. The FSI effect is closely related to the zero-point wave function of $N\bar{N}$ due to the small interaction range for formation compared to that for rescattering. The oscillation-like behavior arises naturally from the Jost function of $N\bar{N}$ caused by FSI, and the “period” of the oscillation is approximately determined by the Yukawa interaction range $1/m_\pi$. As a by-product, our approach can also interpret the threshold enhancement of time-like form factors.

FSI effect with distorted-wave Born approximation.— The separation of the short-range formation and the long-range FSI allows us to study the FSI modification to the production process $e^+e^- \rightarrow N\bar{N}$. It is more intuitive to understand this effect for the time reversal process $N\bar{N} \rightarrow e^+e^-$ since the attractive interaction between $N\bar{N}$ will increase the probability that they meet each other and hence enhance the cross section while the repulsive interaction will suppress it.

The FSI effect can be studied with the distorted-wave Born approximation, and the cross section σ can be expressed with an enhancement or suppression factor $|1/\mathcal{J}|^2$ multiplied by the cross section σ_0 without

FSI [30]:

$$\sigma = \frac{1}{|\mathcal{J}(p)|^2} \sigma_0. \quad (1)$$

$\mathcal{J}(p)$ is the Jost function of final states $N\bar{N}$ with the pure FSI V , and it is closely related to the zero-point wave function.

The radial wave function $\psi_{\ell,p}(r)$ of $N\bar{N}$ can be given by the radial Schrödinger equation for each ℓ partial wave

$$\left(\frac{d^2}{dr^2} - \frac{\ell(\ell+1)}{r^2} - 2\mu V + p^2 \right) \psi_{\ell,p}(r) = 0, \quad (2)$$

where μ is the reduced mass and p is the center-of-mass momentum of $N\bar{N}$ system. In S-wave dominant processes,

$$\mathcal{J}(p) \approx \mathcal{J}_{\ell=0}(p) = \lim_{r \rightarrow 0} \frac{j_0(pr)}{\psi_{0,p}(r)}. \quad (3)$$

$j_0(pr) = \sin(pr)$ is the regular spherical Bessel function. From Eq. (3), this enhancement/suppression factor $|1/\mathcal{J}|^2$ has a well probability interpretation, that is, the ratio of the probability density for finding the scattering state $N\bar{N}$ near the origin with FSI to that without FSI.

The formation of the $N\bar{N}$ pair via virtual photon is of short-range nature, and a naive estimation is $r_0 \sim 1/(2m_N)$. While the interaction range related to $N\bar{N}$ rescattering is approximately given by $a \sim 1/m_\pi$. An estimation $a/r_0 \approx 14$ indicates an explicit separation of formation and rescattering process. We can thus very confidently use the factorized expression in Eq. (1) to study the $e^+e^- \rightarrow N\bar{N}$ reaction.

The interaction range of the annihilation and recreation processes of $N\bar{N}$ is close to r_0 , and they should strongly tangle with the initial formation of the $N\bar{N}$ pair. Thus we put their contribution also into σ_0 , that is, the FSI V does not contain the annihilation potential and therefore we neglect its imaginary part in this work.

The Coulomb interaction between the $N\bar{N}$ pair is weaker and has a much longer interaction range compared to the strong interaction for $N\bar{N}$ rescattering, and this leads to additional well-known Sommerfeld factor $C = |1/S|^2$ with [31]

$$S = \left(\frac{y}{1 - e^{-y}} \right)^{-1/2}, \quad y = \frac{\pi\alpha\sqrt{1 - \beta^2}}{\beta}. \quad (4)$$

Here, α is the electromagnetic fine-structure constant, $\beta = \sqrt{1 - 4m_N^2/s}$ is the center-of-mass velocity of nucleon, and s is the Mandelstam variable. Actually, we can repeat this Coulomb enhancement factor very easily in our approach. Substituting the Coulomb potential in Eq. (2) for V , Eq. (3) is reduced to S by using the non-relativistic approximation $\sqrt{1 - \beta^2} \approx 1$ in the near-threshold region.

TABLE I. Parameters for $p\bar{p}$ and $n\bar{n}$ potentials in Eq. (14).

$N\bar{N}$	a_r (fm)	V_r (MeV)	a (fm)	V_a (MeV)
$p\bar{p}$	0.5	50	1.6	90
$n\bar{n}$	0.5	400	1.4	650

FSI factor with damped oscillation.— As an illustration of the overall FSI effect, firstly we consider the simple case of a rectangular potential well:

$$V(r) = \begin{cases} -V_a & \text{for } 0 \leq r < a \\ 0 & \text{for } r \geq a \end{cases}. \quad (5)$$

We can easily adjust the interaction range a and the potential depth V_a to glimpse some general features of a somehow complicated potential. The Schrödinger equation with this potential have analytical solution. The general solution for $\ell = 0$ is

$$\psi_{0,p}(r) = \begin{cases} \frac{e^{i\delta_0} \sin(p_{in}r)}{\sqrt{\sin^2(p_{in}a) + \frac{p^2}{p_{in}^2} \cos^2(p_{in}a)}} & \text{for } 0 \leq r < a \\ e^{i\delta_0} \sin(pr + \delta_0) & \text{for } r \geq a \end{cases}, \quad (6)$$

where δ_0 is the S-wave phase shift, and

$$p_{in} = \sqrt{p^2 + 2\mu V_a}. \quad (7)$$

We have the enhancement factor

$$|\mathcal{J}(p)| = \sqrt{\frac{p^2}{p_{in}^2} \sin^2(p_{in}a) + \cos^2(p_{in}a)}. \quad (8)$$

The attractive potential gives an enhancement factor as one can easily check that $|1/\mathcal{J}|^2 > 1$ in this model.

Surprisingly this enhancement factor $|1/\mathcal{J}|^2$ is of ‘‘oscillation’’ nature: it reaches its local maximum $|1/\mathcal{J}|_{\max}^2 = 1 + 2\mu V_a/p^2$ when $p_{in}a = n\pi + \pi/2$ and local minimum $|1/\mathcal{J}|_{\min}^2 = 1$ when $p_{in}a = n\pi$. The energy gaps among the 1st, the 2nd, the 3rd and the 4th minimums are:

$$\frac{3\pi^2}{2\mu a^2}, \quad \frac{5\pi^2}{2\mu a^2}, \quad \frac{7\pi^2}{2\mu a^2}. \quad (9)$$

The energy gaps, which show a manifestation of the observed oscillation period, are approximately determined by the interaction range a . Concerning the $N\bar{N}$ scattering, we have $\mu = m_N/2$ and $a \approx 1/m_\pi$, and this gives the 1st gap $\Delta E_1 \approx 0.6$ GeV. It is approximately close to the observed value in experiment.

In addition, the peaks of $|1/\mathcal{J}|^2$ decrease with the increasing energies. This feature describes the damping behavior of the oscillation observed in experiment.

Description for the effective form factor G_{eff} .— It is commonly to express the cross section data in terms of the

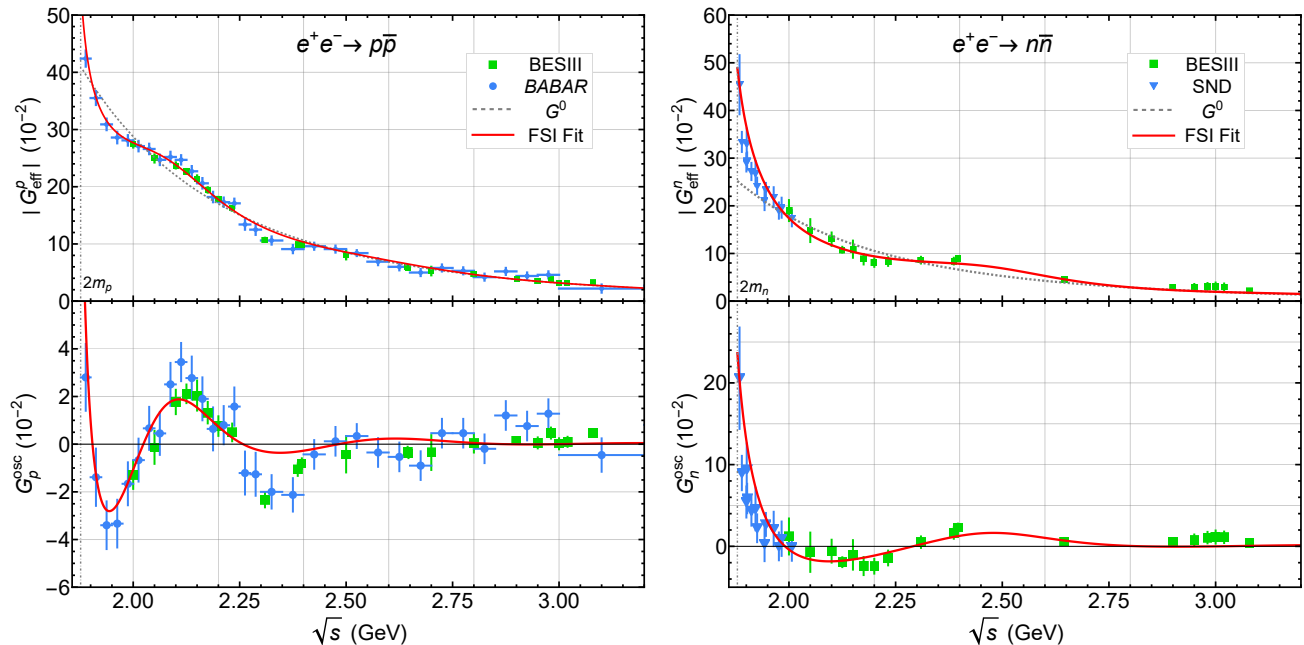


FIG. 1. The effective form factors for protons (left) and neutrons (right) in the time-like region. On the top is the effective form factors $|G_{\text{eff}}|$ while at the bottom is the oscillation part G^{osc} after subtracting the smooth background part G_0 (gray dashed line). The threshold positions $\sqrt{s} = 2m_N$ are labeled as gray dot-dashed vertical lines. In the figure, we only include BESIII [5] (green square) and BABAR [20] (blue circle) data for $p\bar{p}$ and BESIII [21] (green square) and SND [6] (blue triangle) data considering the precision and covering range.

effective form factor which can be obtained as

$$|G_{\text{eff}}(s)| = \sqrt{\frac{3s}{4\pi\alpha^2\beta C(1 + 2m_N^2/s)}} \sigma_{e^+e^- \rightarrow NN}. \quad (10)$$

It can be factorized with the $N\bar{N}$ rescattering correction $1/|\mathcal{J}|$ and the form factor G_0 without FSI:

$$|G_{\text{eff}}(s)| = \frac{1}{|\mathcal{J}|} G_0(s), \quad (11)$$

where G_0 describes the short range production and determines the main feature of G_{eff} in time-like region. Following Ref. [5], it can be parameterized as

$$G_0(s) = \frac{\mathcal{A}}{(1 + s/m_a^2)[1 - s/(0.71 \text{ GeV}^2)]^2}, \quad (12)$$

where $m_a^2 = 7.72 \text{ GeV}^2$ and \mathcal{A} is a constant. With fitted $\mathcal{A}_p = 9.37$ and $\mathcal{A}_n = 5.8$, G_0 can give excellent overall descriptions of effective form factors for nucleons over a wide range. Subtracting the smooth continuum G_0 from $|G_{\text{eff}}|$ we can get the oscillation behavior

$$G^{\text{osc}}(s) = |G_{\text{eff}}| - G_0 = \left(\frac{1}{|\mathcal{J}|} - 1\right) G_0(s). \quad (13)$$

In the previous section we have shown that a simple rectangular potential well already leads to an oscillation feature, and the enhancement factor is larger than 1 in

that case, which means G^{osc} will be positive with the attractive interaction. To obtain the observed oscillatory structure, we need the potential to be a bit more complicated by taking

$$V(r) = \begin{cases} -V_r & 0 \leq r < a_r \\ -V_a & a_r \leq r < a \\ 0 & r \geq a \end{cases}, \quad (14)$$

where $0 < V_r < V_a$ and we take $a_r = 0.5 \text{ fm}$.

We show the FSI effect with such potentials on the $p\bar{p}$ and $n\bar{n}$ effective form factors in Fig. 1. The corresponding parameters are listed in Table. I. The overall oscillatory behavior are nicely reproduced due to the FSI effect with the interaction range a about $1.4 \sim 1.6 \text{ fm}$.

The details of describing the effective form factors rely on the choices of the continuum part G_0 , which we still do not understand very well because the formation process involves the complicated hadronization and other difficulties. Possibly, better descriptions can be achieved for $|G_{\text{eff}}|$ by using different G_0 rather than same as the experiment collaborations.

Threshold enhancement of time-like form factors— From Fig. 1, one notices that the neutron effective form factor has stronger near-threshold enhancement than that for proton. The SND measurement observed the enhancement for the neutron cross section just above threshold at $\sqrt{s} - 2m_n \approx 5 \text{ MeV}$ [6], which contradicts naive phase

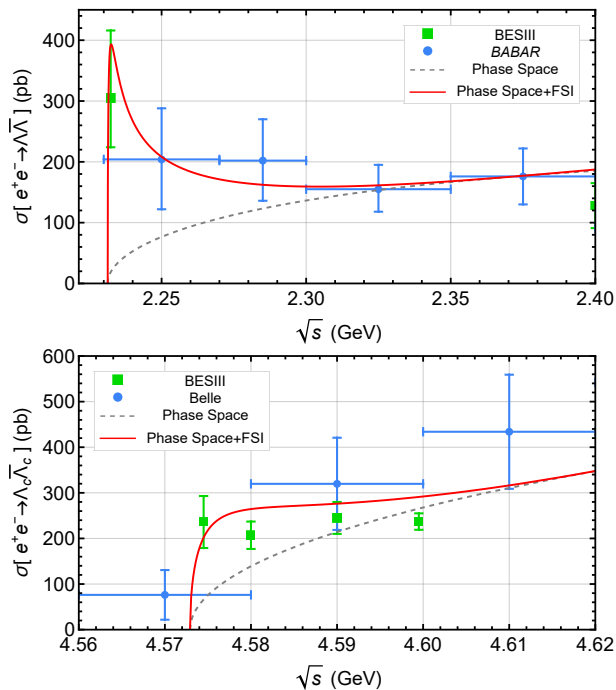


FIG. 2. The cross sections near thresholds for $e^+e^- \rightarrow \Lambda\bar{\Lambda}$ [32, 47] and $e^+e^- \rightarrow \Lambda_c\bar{\Lambda}_c$ [33, 48]. The threshold data deviate far away from the fits (dashed lines) proportional to phase space distributions. The fits (solid lines) improve after including the FSI enhancement factor given by Eq. (8) with $a = 1/m_\pi$ and appropriately adjusted V_0 .

space expectation. Our approach can easily provide such enhancement as seen in Fig. 1. The reason is that the FSI factor near the threshold $1/|\mathcal{J}|_{p \rightarrow 0} \rightarrow 1/\cos^2(\sqrt{2\mu V_a}a)$ with an attractive squared-well potential. With appropriate V_a and a , $1/|\mathcal{J}|_{p \rightarrow 0}$ can give rise to very large enhancement near-threshold.

In addition to $N\bar{N}$ production, other baryon-antibaryon pair productions near thresholds have also been measured [32–37]. Abnormally large cross sections are observed in $e^+e^- \rightarrow \Lambda\bar{\Lambda}$ near the threshold ($\sqrt{s} - 2m_\Lambda \approx 1$ MeV [32] and possibly $e^+e^- \rightarrow \Lambda_c\bar{\Lambda}_c$ at ($\sqrt{s} - 2m_{\Lambda_c} \approx 1.58$ MeV [33]. However, no such phenomenon were found in the $\Xi\bar{\Xi}$ [34, 35] and $\Sigma\bar{\Sigma}$ [36, 37] productions. These have been studied with various approaches [38–46]. Our framework can provide a naturally unified explanation for the near-threshold enhancements either large or almost none, which relies on the different FSI between these baryon-antibaryon pairs. We can fit the enhanced cross sections near thresholds for productions of $\Lambda\bar{\Lambda}$ and $\Lambda_c\bar{\Lambda}_c$ nicely with simple squared-well potentials as shown in Fig. 2.

Summary.— We have introduced a simple framework to deal with the damped oscillation observed in the electromagnetic form factors of nucleons which is measured in $e^+e^- \rightarrow N\bar{N}$. The FSI effect is important for this phenomenon and leads to a factor made of the $N\bar{N}$ Jost func-

tion with the distorted-wave Born approximation. Using the squared-well potentials, the FSI factors are naturally damped oscillatory and the experimental data can be well explained. It can easily extend to interpret the threshold enhancements on the production cross sections for the $n\bar{n}$, $\Lambda\bar{\Lambda}$, and $\Lambda_c\bar{\Lambda}_c$, and moreover, same approach can also give inapparent enhancements in other channels just with a proper adjustment of FSI parameters.

The oscillation phenomenon could also exist in the productions of hyperon-antihyperon and other pairs, which is an interesting topic in both experiment and theory [49]. With the better understanding of the form factors in future, we hope one can furthermore disclose the related structures of nucleons and other baryons.

Z.-W. Liu thanks for useful discussion with Prof. Anthony W. Thomas and Derek B. Leinweber. This work is supported by the China National Funds for Distinguished Young Scientists under Grant No. 11825503, National Key Research and Development Program of China under Contract No. 2020YFA0406400, the 111 Project under Grant No. B20063, and the National Natural Science Foundation of China under Grant Nos. 12175091, 11965016, 12047501 and U2032109.

* qianrq18@lzu.edu.cn

† liuzhanwei@lzu.edu.cn

‡ caoxu@impcas.ac.cn

§ xiangliu@lzu.edu.cn

- [1] A. J. R. Puckett *et al.*, Final Analysis of Proton Form Factor Ratio Data at $Q^2 = 4.0, 4.8$ and 5.6 GeV², *Phys. Rev. C* **85**, 045203 (2012), arXiv:1102.5737 [nucl-ex].
- [2] A. J. R. Puckett *et al.*, Polarization Transfer Observables in Elastic Electron Proton Scattering at $Q^2 = 2.5, 5.2, 6.8$, and 8.5 GeV², *Phys. Rev. C* **96**, 055203 (2017), [Erratum: *Phys.Rev.C* 98, 019907 (2018)], arXiv:1707.08587 [nucl-ex].
- [3] J. P. Lees *et al.* (BaBar), Study of $e^+e^- \rightarrow p\bar{p}$ via initial-state radiation at BABAR, *Phys. Rev. D* **87**, 092005 (2013), arXiv:1302.0055 [hep-ex].
- [4] J. P. Lees *et al.* (BaBar), Measurement of the $e^+e^- \rightarrow p\bar{p}$ cross section in the energy range from 3.0 to 6.5 GeV, *Phys. Rev. D* **88**, 072009 (2013), arXiv:1308.1795 [hep-ex].
- [5] M. Ablikim *et al.* (BESIII), Measurement of proton electromagnetic form factors in $e^+e^- \rightarrow p\bar{p}$ in the energy region 2.00 - 3.08 GeV, *Phys. Rev. Lett.* **124**, 042001 (2020), arXiv:1905.09001 [hep-ex].
- [6] M. N. Achasov *et al.* (SND), Experimental study of the $e^+e^- \rightarrow n\bar{n}$ process at the VEPP-2000 e^+e^- collider with the SND detector, *Eur. Phys. J. C* **82**, 761 (2022), arXiv:2206.13047 [hep-ex].
- [7] T. Massam and A. Zichichi, A one-parameter fit to the electromagnetic form factors of the nucleon, *Il Nuovo Cimento A Series 10* **43**, 1137 (1966).
- [8] F. Iachello and Q. Wan, Structure of the nucleon from electromagnetic timelike form factors, *Phys. Rev. C* **69**, 055204 (2004).

- [9] R. Bijker and F. Iachello, Re-analysis of the nucleon space- and time-like electromagnetic form-factors in a two-component model, *Phys. Rev. C* **69**, 068201 (2004), [arXiv:nucl-th/0405028](#).
- [10] Q. Wan and F. Iachello, A unified description of baryon electromagnetic form factors, *Int. J. Mod. Phys. A* **20**, 1846 (2005).
- [11] E. L. Lomon and S. Pacetti, Time-like and space-like electromagnetic form factors of nucleons, a unified description, *Phys. Rev. D* **85**, 113004 (2012), [Erratum: *Phys.Rev.D* 86, 039901 (2012)], [arXiv:1201.6126 \[hep-ph\]](#).
- [12] Y.-H. Lin, H.-W. Hammer, and U.-G. Meißner, New insights into the nucleon's electromagnetic structure, (2021), [arXiv:2109.12961 \[hep-ph\]](#).
- [13] Y.-H. Lin, H.-W. Hammer, and U.-G. Meißner, Dispersion-theoretical analysis of the electromagnetic form factors of the nucleon: Past, present and future, *Eur. Phys. J. A* **57**, 255 (2021), [arXiv:2106.06357 \[hep-ph\]](#).
- [14] V. A. Matveev, R. M. Muradyan, and A. N. Tavkhelidze, Automodelity in strong interactions, *Teor. Mat. Fiz.* **15**, 332 (1973).
- [15] S. J. Brodsky and G. R. Farrar, Scaling Laws at Large Transverse Momentum, *Phys. Rev. Lett.* **31**, 1153 (1973).
- [16] J. Gasser, M. E. Sainio, and A. Svarc, Nucleons with Chiral Loops, *Nucl. Phys. B* **307**, 779 (1988).
- [17] B. Kubis and U.-G. Meißner, Low-energy analysis of the nucleon electromagnetic form-factors, *Nucl. Phys. A* **679**, 698 (2001), [arXiv:hep-ph/0007056](#).
- [18] V. Bernard, N. Kaiser, and U.-G. Meißner, Nucleon electroweak form-factors: Analysis of their spectral functions, *Nucl. Phys. A* **611**, 429 (1996), [arXiv:hep-ph/9607428](#).
- [19] S. Pacetti, R. Baldini Ferroli, and E. Tomasi-Gustafsson, Proton electromagnetic form factors: Basic notions, present achievements and future perspectives, *Phys. Rept.* **550-551**, 1 (2015).
- [20] A. Bianconi and E. Tomasi-Gustafsson, Periodic interference structures in the timelike proton form factor, *Phys. Rev. Lett.* **114**, 232301 (2015), [arXiv:1503.02140 \[nucl-th\]](#).
- [21] M. Ablikim *et al.* (BESIII), Oscillating features in the electromagnetic structure of the neutron, *Nature Phys.* **17**, 1200 (2021).
- [22] J. P. B. C. de Melo, T. Frederico, E. Pace, S. Pisano, and G. Salme, Time- and Spacelike Nucleon Electromagnetic Form Factors beyond Relativistic Constituent Quark Models, *Phys. Lett. B* **671**, 153 (2009), [arXiv:0804.1511 \[hep-ph\]](#).
- [23] X. Cao, J.-P. Dai, and H. Lenske, Timelike nucleon electromagnetic form factors: All about interference of isospin amplitudes, *Phys. Rev. D* **105**, L071503 (2022), [arXiv:2109.15132 \[hep-ph\]](#).
- [24] I. T. Lorenz, H. W. Hammer, and U. G. Meißner, New structures in the proton-antiproton system, *Phys. Rev. D* **92**, 034018 (2015), [arXiv:1506.02282 \[hep-ph\]](#).
- [25] A. Bianconi and E. Tomasi-Gustafsson, Phenomenological analysis of near threshold periodic modulations of the proton timelike form factor, *Phys. Rev. C* **93**, 035201 (2016), [arXiv:1510.06338 \[nucl-th\]](#).
- [26] Q.-H. Yang, L.-Y. Dai, D. Guo, J. Haidenbauer, X.-W. Kang, and U.-G. Meißner, New insights into the oscillation of the nucleon electromagnetic form factors, (2022), [arXiv:2206.01494 \[nucl-th\]](#).
- [27] A. Bianconi and E. Tomasi-Gustafsson, Fourth dimension of the nucleon structure: Spacetime analysis of the timelike electromagnetic proton form factors, *Phys. Rev. C* **95**, 015204 (2017), [arXiv:1611.02149 \[hep-ph\]](#).
- [28] A. Bianconi and E. Tomasi-Gustafsson, Soft rescattering in the timelike proton form factor within a spacetime scheme, *Phys. Rev. C* **98**, 055204 (2018), [arXiv:1809.05709 \[nucl-th\]](#).
- [29] A. I. Milstein and S. G. Salnikov, $N\bar{N}$ production in e^+e^- annihilation near the threshold revisited, (2022), [arXiv:2207.14020 \[hep-ph\]](#).
- [30] J. R. Taylor, *Scattering Theory: The Quantum Theory on Nonrelativistic Collisions, Chapter 21-b* (John Wiley & Sons, New York, 1972).
- [31] A. B. Arbuzov and T. V. Kopylova, On relativization of the Sommerfeld-Gamow-Sakharov factor, *JHEP* **04**, 009, [arXiv:1111.4308 \[hep-ph\]](#).
- [32] M. Ablikim *et al.* (BESIII), Observation of a cross-section enhancement near mass threshold in $e^+e^- \rightarrow \Lambda\bar{\Lambda}$, *Phys. Rev. D* **97**, 032013 (2018), [arXiv:1709.10236 \[hep-ex\]](#).
- [33] M. Ablikim *et al.* (BESIII), Precision measurement of the $e^+e^- \rightarrow \Lambda_c^+ \bar{\Lambda}_c^-$ cross section near threshold, *Phys. Rev. Lett.* **120**, 132001 (2018), [arXiv:1710.00150 \[hep-ex\]](#).
- [34] M. Ablikim *et al.* (BESIII), Measurement of cross section for $e^+e^- \rightarrow \Xi^- \bar{\Xi}^+$ near threshold at BESIII, *Phys. Rev. D* **103**, 012005 (2021), [arXiv:2010.08320 \[hep-ex\]](#).
- [35] M. Ablikim *et al.* (BESIII), Measurement of cross section for $e^+e^- \rightarrow \Xi^0 \bar{\Xi}^0$ near threshold 10.1016/j.physletb.2021.136557 (2021), [arXiv:2105.14657 \[hep-ex\]](#).
- [36] M. Ablikim *et al.* (BESIII), Measurements of Σ^+ and Σ^- time-like electromagnetic form factors for center-of-mass energies from 2.3864 to 3.0200 GeV, *Phys. Lett. B* **814**, 136110 (2021), [arXiv:2009.01404 \[hep-ex\]](#).
- [37] M. Ablikim *et al.* (BESIII), Measurement of the $e^+e^- \rightarrow \Sigma^0 \bar{\Sigma}^0$ cross sections at center-of-mass energies from 2.3864 to 3.0200 GeV, *Phys. Lett. B* **831**, 137187 (2022), [arXiv:2110.04510 \[hep-ex\]](#).
- [38] V. F. Dmitriev and A. I. Milstein, Final state interaction effects in the $e^+e^- \rightarrow N\bar{N}$ process near threshold, *Phys. Lett. B* **658**, 13 (2007).
- [39] V. F. Dmitriev, A. I. Milstein, and S. G. Salnikov, Isoscalar amplitude dominance in e^+e^- annihilation to $N\bar{N}$ pair close to the threshold, *Phys. Atom. Nucl.* **77**, 1173 (2014), [arXiv:1307.0936 \[hep-ph\]](#).
- [40] Z.-Y. Li, A.-X. Dai, and J.-J. Xie, Electromagnetic form factors of Λ hyperon in the vector meson dominance model and the near-threshold enhancement of the $e^+e^- \rightarrow \Lambda\bar{\Lambda}$ reaction, (2021), [arXiv:2107.10499 \[hep-ph\]](#).
- [41] J. Haidenbauer, X. W. Kang, and U. G. Meißner, The electromagnetic form factors of the proton in the timelike region, *Nucl. Phys. A* **929**, 102 (2014), [arXiv:1405.1628 \[nucl-th\]](#).
- [42] J. Haidenbauer, C. Hanhart, X.-W. Kang, and U.-G. Meißner, Origin of the structures observed in e^+e^- annihilation into multipion states around the $\bar{p}p$ threshold, *Phys. Rev. D* **92**, 054032 (2015), [arXiv:1506.08120 \[nucl-th\]](#).
- [43] X. Cao, J.-P. Dai, and Y.-P. Xie, Vector mesons and electromagnetic form factor of the Λ hyperon, *Phys. Rev. D* **98**, 094006 (2018), [arXiv:1808.06382 \[hep-ph\]](#).
- [44] Y. Yang, D.-Y. Chen, and Z. Lu, Electromagnetic form factors of Λ hyperon in the vector meson dom-

- inance model, *Phys. Rev. D* **100**, 073007 (2019), [arXiv:1902.01242 \[hep-ph\]](#).
- [45] J. Haidenbauer, U.-G. Meißner, and L.-Y. Dai, Hyperon electromagnetic form factors in the timelike region, *Phys. Rev. D* **103**, 014028 (2021), [arXiv:2011.06857 \[nucl-th\]](#).
- [46] L.-Y. Dai, J. Haidenbauer, and U. G. Meißner, Re-examining the $X(4630)$ resonance in the reaction $e^+e^- \rightarrow \Lambda_c^+\bar{\Lambda}_c^-$, *Phys. Rev. D* **96**, 116001 (2017), [arXiv:1710.03142 \[hep-ph\]](#).
- [47] B. Aubert *et al.* (BaBar), Study of $e^+e^- \rightarrow \Lambda\bar{\Lambda}$, $\Lambda\bar{\Sigma}^0$, $\Sigma^0\bar{\Sigma}^0$ using initial state radiation with BABAR, *Phys. Rev. D* **76**, 092006 (2007), [arXiv:0709.1988 \[hep-ex\]](#).
- [48] G. Pakhlova *et al.* (Belle), Observation of a near-threshold enhancement in the $e^+e^- \rightarrow \Lambda_c^+\Lambda_c^-$ cross section using initial-state radiation, *Phys. Rev. Lett.* **101**, 172001 (2008), [arXiv:0807.4458 \[hep-ex\]](#).
- [49] A.-X. Dai, Z.-Y. Li, L. Chang, and J.-J. Xie, Electromagnetic form factors of neutron, Λ and Σ^0 in the oscillating view of point, (2021), [arXiv:2112.06264 \[hep-ph\]](#).